550.342 : 550.373 (581)

Upper mantle seismic wave velocities in the Hindukush region

A. N. TANDON

Meteorological Office, New Delhi

(Received 17 December 1966)

ABSTRACT. Gutenberg's method has been applied for the determination of the seismic wave velocities and their variations with depth in the upper part of the upper mantle below the Hindukush mountains. Data from fifty earthquakes occurring at various depths in the Hindukush region have been utilised. The results confirm the existence of a low velocity layer for S-waves at a depth of about 160 km below the surface. The S-velocity decreases slowly from a value of 4·5 km/sec at a depth of 65 km to a value of 4·4 km/sec at a depth of 160 km after which it rises again reaching value of 4·52 km/sec at a depth of 225 km. No such velocity minima is, however, discernible in the case of P-waves. The velocity of P-waves appears to remain nearly constant at 8 km/sec upto a depth of 160 km. It then rises steeply up to a depth of 200 km after which the velocity gradient decreases. The value of Poisson's ratio just below the Mohorovicic discontinuity in this region works out to be 0·26. This value increases steadily to 0·29 upto a depth of 225 km and then attains a constant value.

1. Introduction

According to the Herglotz-Wiechert method of tracing the paths of seismic rays

$$(v_r.\ R)/r = \bar{v}/\sin i_r \qquad (1)$$

where v_r is the true velocity of the wave at its deepest point at a distance r from the centre of the earth, i_r is the angle of incidence made by the ray emerging at the surface of the earth, and R the radius of the earth. $\bar{v}$ is the true velocity at the surface of the earth and, therefore, $\bar{v}/\sin i_r$ is the apparent surface velocity V at the terminus of the ray :

$$V = (v_r.\ R)/r \qquad (2)$$

Seismic rays leaving the focus of an earthquake at various angles of incidence will appear at the surface of the earth at different distances. Of all these rays, the ray leaving the focus horizontally will appear at a particular distance $\triangle$. At this point the travel-time curve will have a point of inflexion and the apparent velocity will have its minimum value V^*, which can be found with the help of the observed travel-time curve. The relation (2) can be used to determine the true velocity V_r at the focus.

$$\begin{aligned} V_r &= V^*.r/R \\ \text{Since} \quad r &= (R-h) \\ V_r &= V^*(R-h)/R \\ &= V^*(1-h/R) \end{aligned} \qquad (3)$$

This method can, however, be applied only under limited conditions. If the velocity increases continuously with depth the ray will always be concave to the surface and will also have a vertex. In this case the time-distance curve will also be continuous. Difficulty will, however, arise if at some depth the velocity instead of increasing starts decreasing with depth. In such a case the ray leaving the focus horizontally will deflect towards the centre of the earth and may not emerge at the surface under certain circumstances. In other words the presence of a low velocity layer may create a shadow zone at the surface. It can be shown that even in the presence of a low velocity layer, the ray would emerge at the surface if the velocity does not decrease at a rate greater than given by

$$dV_r/dr = V_r/r \qquad (4)$$

The relation (3) was used by Gutenberg (1953) to calculate the velocities of P and S waves in the interior of the earth upto a depth of nearly 600 km. Using data of 82 earthquakes with epicentre mostly in the Japan area he computed curves for P and S velocites and also for the value of the Poisson's ratio σ as a function of depth. His results showed that the velocities of both P and S show a decrease below the Mohorovicic discontinuity with a minimum around h =100 km for P waves and h=150 km for S waves. Poisson's ratio increased from a value of 0·26 at a depth of 50 km to 0·29 at a depth of 250 km and became constant thereafter.

In view of the lateral inhomogenities in the earth's crust and upper mantle it was decided to apply this method to study the variation of velocities with depth in the Hindukush region which is tectonically considered a very important area. It is a perenial source of large and small earthquakes occurring mostly at a depth of about 225 km and from nearly the same focus. Earthquakes also originate at depth less than 250 km at places within a few degrees from this source.

2. Method and materials

The method used was almost the same as used by Gutenberg with only minor modifications in detail. Data of 50 earthquakes occurring at different depths in the Hindukush region was collected

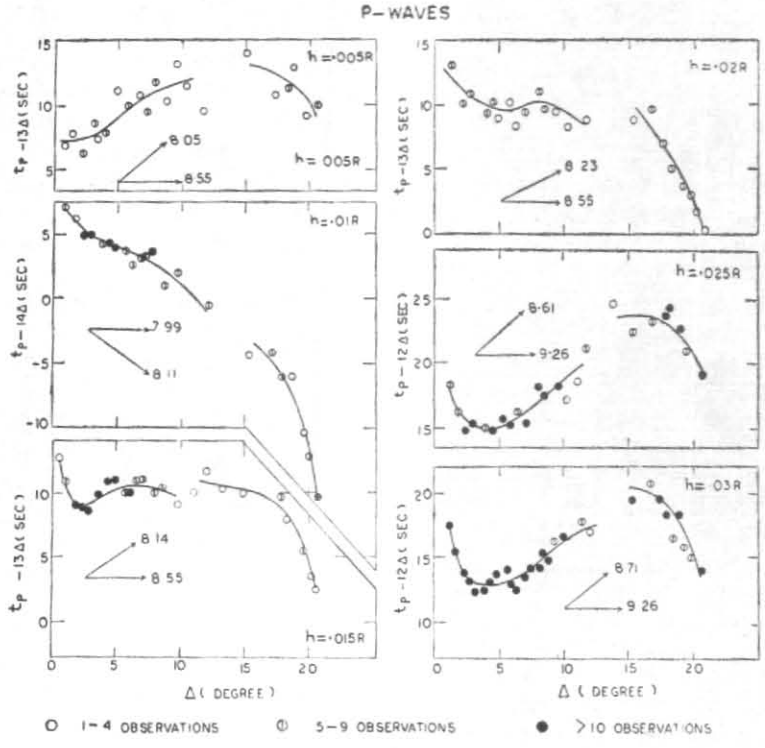
P-WAVES
h=·005R
h=·01R
h=·015R
h=·02R
h=·025R
h=·03R
8·05
8·55
7·99
8·11
8·14
8·55
8·23
8·55
8·61
9·26
8·71
9·26
Δ (DEGREE)
O 1-4 OBSERVATIONS ⊕ 5-9 OBSERVATIONS ● >10 OBSERVATIONS

Fig. 1(a)

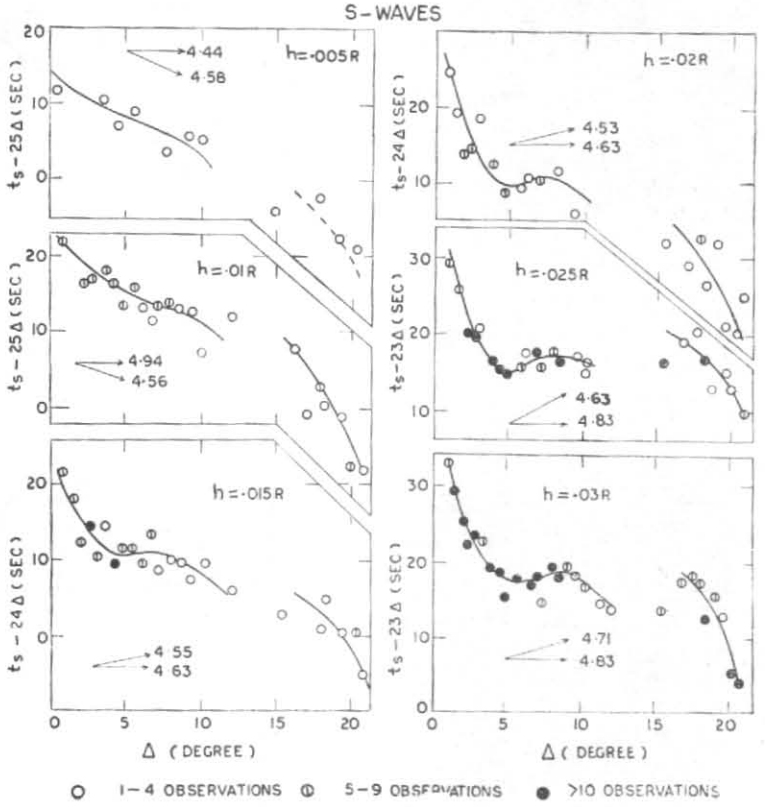
S-WAVES
h=·005R
h=·01R
h=·015R
h=·02R
h=·025R
h=·03R
4·44
4·58
4·94
4·56
4·55
4·63
4·53
4·63
4·63
4·83
4·71
4·83
Δ (DEGREE)
O 1-4 OBSERVATIONS ⊕ 5-9 OBSERVATIONS ● >10 OBSERVATIONS

Fig. 1(b)

from the International Seismological Summaries (1949 to 1958). Relevant particulars of these are given in Table 1. A good network of Russian, Chinese and Indian stations has been existing around the Hindukush source for quite some time and hence there was no difficulty in getting the necessary data of P and S times and depth of focus at epicentral distances close to the epicentre to about $\triangle = 20°$. The parameters regarding these earthquakes as given in the I.S.S. were used as such without any modifications. Only in a few cases the depth was checked but no modification was found necessary. All observations for which the P residuals exceeded 4 sec and the S residuals 8 sec were left out. Instead of plotting travel times of waves against the distance, the reduced travel times were used, as done by Gutenberg, because they bring about the point of inflexion of the T–D curve more clearly. Reduced travel time is the actual travel time diminished by the product of distance and a constant. The value of the constant is so chosen that the reduced travel time is approximately the same near the point of inflexion in the curve. Gutenberg had plotted the reduced T–D curves for each earthquake individually for calculation of the true velocities at depths. In this case, however, the observations of all earthquakes occurring within 10 km of a specified depth were combined. In order to smoothen out the curves, travel time readings for distances occurring within about 50 km were also combined, and ultimately points representing the weighted averages of distances and travel times were calculated and plotted. In this way the reduced T–D curves for values of $h = \cdot 005, \cdot 01, \cdot 015, \cdot 02, \cdot 025$ and $\cdot 03\ R$ were plotted from which the apparent velocities were obtained. The weighted average of distances and reduced travel times, the number of observations used for each point are given in Table 2. The number of observations available for depths of $\cdot 025$ and $\cdot 03\ R$ were considerably larger than available for other depths.

3. Results

Figs. 1 (a) and 1(b) give the reduced T-D curves for the various depths for the P and S waves. Calculated values of the apparent velocities, the true velocities of the P and S waves and the computed value of the Poisson's ratio at these depths are given in Table 3 and shown in Fig. 2. The depth $h = \cdot 005\ R$ corresponds to about 65 km, which is about the depth of the Mohorovicic discontinuity in this region (Reznichenco and Kosminskaya 1964). It will be seen from the curves in Fig. 2 that the velocity of the P wave is almost constant at 8 km/sec upto a depth of nearly 160 km. At this depth it rises steeply upto about 200 km after which the velocity gradient decreases. The S velocity decreases slowly from a value of about 4·52 km at a depth of 65 km to a value of 4·40 km/sec at a depth of 160 km after which it rises again, reaching a value of 4·52 km/sec at a depth of 225 km. Thus the low velocity channel for S below the Mohorovicic discontinuity is more clearly marked than for P waves. The value of the Poisson's ratio just below the Mohorovicic discontinuity in this region, *i. e.*, at a depth of 65 km below the earth's surface works out to be 0·26. As the depth increases, this value rises steadily to nearly 0·29 at a depth of 225 km, a result consistent with the findings of Gutenberg. The larger velocity decrease of S waves compared to the P waves suggests that the value of the coefficient of rigidity decreases more rapidly upto a depth of 160 km than the bulk modulus.

The travel times of both P and S waves for all the depths investigated do not indicate any shadow zone for distances upto 10°. Very few observations were, however, available for distances between 10° and 15° particularly between 12° and 15°. Whether this was due to lack of proper observing stations at these distances or due to the existence of a shadow zone, could not be investigated. It can, however, be noticed that the lack of observations in the range $\triangle = 10°$ to 15° is more predominant in the case of S waves.

The reduced travel-time curves for all the depths are continuous for distances upto $\triangle = 12°$, and again between $\triangle = 15°$ to 20°. It has already been mentioned earlier that there was lack of observations in the range $\triangle = 10°$ to $\triangle = 15°$. Inspite of this handicap it is seen from the trend of T–D curve that they are not continuous within this range and are offset by a few seconds with respect to the earlier branch. The travel times in this range ($\triangle = 15°$ to $\triangle = 20°$) agree within two seconds of those given in *J and B Tables* (1948), both for P as well as S.

Dowling and Nuttli (1964) constructed a number of travel-time curves for a surface focus with the help of a 1620 computor on the basis of the Herglotz-Wiechert relation and assuming the presence of a low velocity channel in the upper mantle. Various earth models having different velocity gradients, depth channel, and channel width were tried. The results were also compared with the observed travel times for two atomic explosions. One of their conclusions was that inspite of the presence of a low velocity channel there may not exist a shadow zone provided the velocity increases rapidly enough below the channel. In the presence of a low velocity channel the travel-time curve consists of three branches. Rays which have their point of deepest penetration above the top of the low velocity channel lie on a continuous curve terminating at a point with $\triangle$ equal to about 10 to 12°. At this point there is a discontinuity in the T–D curve and rays leaving the focus at smaller angles

TABLE 1

Serial No.	Date	Time of origin			Epicentre		h (km)
		h	m	s	Lat. (°N)	Long. (°E)	
1	1 May 1953	21	18	19	33·7	72·5	65
2	30 Aug 1957	16	18	03	39·34	72·88	56
3	6 Jan 1958	01	54	39	36·97	71·09	78
4	28 Jan 1951	10	20	08	36·9	70·8	96
5	12 Jul 1953	00	53	10	36·5	71·0	96
6	3 Jul 1955	14	01	55	36·8	71·0	96
7	13 Oct 1956	08	21	12	36·32	71·28	96
8	1 Sep 1957	12	50	03	39·03	74·34	87
9	20 Jan 1957	18	12	47	36·72	71·28	91
10	4 Jan 1951	03	38	22	38·4	73·6	128
11	1 Jul 1952	17	59	51	36·8	71·4	128
12	21 Dec 1952	08	10	18	36·8	71·4	128
13	26 Feb 1954	18	46	18	36·8	71·4	128
14	6 Mar 1955	20	55	27	38·1	72·9	128
15	29 May 1958	03	15	59	37·66	72·19	121
16	10 Dec 1958	03	43	43	36·35	71·28	111
17	10 May 1949	09	13	26	36·7	70·5	160
18	27 Nov 1952	07	20	31	36·6	70·1	160
19	16 May 1954	20	10	39	36·6	70·9	160
20	18 Sep 1958	20	53	04	36·49	70·70	157
21	14 Mar 1952	23	27	12	37·0	77·2	192
22	11 Apr 1954	10	53	32	36·4	70·8	192
23	7 Aug 1954	15	13	44	36·4	70·7	192
24	24 Mar 1957	12	05	16	36·55	70·92	194
25	7 Mar 1958	06	55	32	36·55	70·68	202
26	28 Mar 1958	12	06	24	36·51	70·98	188
27	30 Apr 1958	08	16	48	36·53	70·95	186
28	8 Aug 1958	12	52	09	36·64	71·04	201
29	7 Dec 1947	01	44	20	36·7	70·5	224
30	9 Jan 1948	14	52	27	36·5	71·0	224
31	4 Mar 1949	10	19	30	36·7	70·5	224
32	6 Jan 1951	05	17	20	36·5	71·0	224
33	16 Jan 1951	08	08	42	36·7	70·5	224
34	12 Jun 1951	22	40	39	36·3	71·0	224
35	19 Aug 1951	15	38	46	36·9	70·8	224
36	4 Oct 1951	05	43	08	36·7	70·5	224
37	15 Oct 1951	14	48	59	36·7	70·5	224
38	7 Jun 1952	16	01	23	36·7	70·5	224
39	5 Jul 1952	17	19	51	36·7	70·5	224
40	18 Oct 1952	21	26	19	36·7	70·5	224
41	5 Nov 1953	08	21	39	36·7	70·5	224
42	10 Jul 1954	22	56	54	36·6	71·1	224
43	16 Mar 1955	20	39	39	36·7	70·3	224
44	14 May 1955	13	35	43	36·6	71·3	224
45	6 Apr 1956	07	11	38	36·4	70·7	224
46	3 Jul 1956	23	26	17	36·6	71·1	224
47	20 Aug 1957	15	21	09	37·67	71·24	227
48	17 Feb 1958	05	18	42	36·50	70·68	210
49	28 Mar 1958	04	09	36	36·39	71·02	232
50	25 Sep 1958	06	54	64	36·59	70·11	219

TABLE 2

P			*S*			*P*			*S*			*P*			*S*		
$\overline{\Delta}$ (°)	$\overline{t}$ (sec)	No. of obs.	$\overline{\Delta}$ (°)	$\overline{t}$ (sec)	No. of obs.	$\overline{\Delta}$ (°)	$\overline{t}$ (sec)	No. of obs.	$\overline{\Delta}$ (°)	$\overline{t}$ (sec)	No. of obs.	$\overline{\Delta}$ (°)	$\overline{t}$ (sec)	No. of obs.	$\overline{\Delta}$ (°)	$\overline{t}$ (sec)	No. of obs.
	$h=\cdot005R$						$h=\cdot01R$						$h=\cdot015R$				
0·70	16·0	1	0·65	28·0	1	0·96	20·2	5	1·0	37·0	5	0·65	21·2	4	0·68	37·6	5
1·40	26·0	1	3·61	100·7	4	1·55	27·7	4	2·38	66·3	9	1·06	24·6	3	1·37	50·81	7
2·30	36·6	6	4·6	122·0	2	2·35	37·7	14	2·80	77·0	5	1·81	32·5	10	2·09	62·7	9
3·08	48·6	6	5·7	151·5	2	2·75	43·2	20	3·82	103·6	5	2·40	40·1	18	2·57	73·6	22
3·40	51·6	3	6·5	163·0	1	3·76	56·7	7	4·40	116·7	9	2·88	45·9	17	3·11	85·2	8
3·92	59·5	6	7·90	201·7	4	4·32	64·7	14	4·97	127·8	4	3·62	57·0	16	3·60	101·0	2
4·87	74·5	4	9·25	237·0	2	4·77	70·6	10	5·70	148·4	5	4·41	66·1	12	4·25	113·5	12
5·68	83·6	7	10·1	257·3	3	5·51	79·6	9	6·23	159·0	3	4·95	75·3	11	4·83	127·1	8
6·73	98·3	3	14·9	368·5	2	6·12	88·2	6	6·90	174·0	4	5·55	82·0	8	5·50	143·3	7
7·38	105·4	5	17·95	447·5	2	6·80	98·3	6	7·34	187·2	5	6·04	88·4	11	6·05	155·0	6
7·94	114·1	7	18·85	459·5	2	7·25	104·8	8	8·06	205·5	5	6·57	96·3	7	6·65	173·0	5
8·90	126·0	4	19·4	477·3	3	8·03	115·9	11	8·60	218·0	2	7·10	103·3	7	7·15	180·5	2
9·50	136·6	3	20·4	501·0	4	8·62	121·6	5	9·40	237·7	4	8·01	114·0	9	8·10	204·3	3
10·20	144·0	4				9·54	135·4	5	10·15	251·0	2	8·65	122·7	7	8·57	217·7	4
11·60	160·3	3				11·9	166·0	1	12·60	317·0	1	9·80	136·5	1	9·40	233·0	3
15·00	209·0	1				15·1	207·0	1	16·20	403·0	1	11 10	154·3	3	10·33	251·3	3
17·30	235·6	3				16·94	233·0	5	17·10	417·0	1	12·10	169·0	3	12·0	294·0	1
18·02	245·4	5				17·75	242·5	6	17·87	439·7	4	13·45	185·0	2	17·9	430·5	4
18·75	255·5	2				18·50	253·0	3	18·18	445·0	3	15·0	205·0	1	18·3	444·0	2
19·60	264·0	2				19·42	261·5	4	19·35	472·5	4	17·76	240·6	5	19·42	466·5	4
20·51	276·6					19·9	266·4	7	20·10	485·0	5	18·16	244·0	3	20·15	485·6	8
						20·64	273·6	5	20·8	502·0	1	19·7	261·6	8	20·7	490·6	3
												20·25	266·7	4			
												20·65	271·0	4			
	$h=\cdot02R$						$h=\cdot025R$						$h=\cdot03R$				
1·34	30·6	5	1·1	51·0	1	1·20	32·6	8	1·13	55·5	6	1·15	33·6	19	1·10	58·1	9
2·31	40·1	9	1·56	57·0	3	1·71	36·3	7	1·58	62·2	5	1·66	37·7	10	1·48	63·1	10
2·77	47·3	7	2·28	68·7	6	2·46	44·2	28	2·39	75·2	17	2·27	43·4	41	2·09	73·1	13
4·09	62·4	8	2·61	77·5	7	2·85	49·4	21	2·74	82·5	22	2·67	48·5	50	2·45	78·5	40
4·58	69·7	9	3·10	91·0	2	3·95	62·4	8	3·2	94·0	2	3·17	52·8	11	2·78	87·9	22
4·95	73·2	4	4·12	111·2	5	4·44	68·0	20	3·95	107·6	8	3·94	62·3	28	3·38	100·2	5
5·76	85·0	3	4·80	124·1	7	5·03	76·0	14	4·49	118·5	20	4·42	68·4	43	3·96	110·2	20
6·45	92·2	4	5·83	149·6	3	5·91	86·0	10	4·95	128·8	11	4·84	74·2	23	4·47	121·1	43
7·10	101·7	9	6·35	163·0	2	6·40	94·9	8	5·86	150·4	5	5·54	82·9	11	4·94	128·8	11
8·12	116·6	5	7·02	179·0	6	7·18	101·4	25	6·26	161·6	4	5·92	86·4	16	5·73	149·5	14
8·63	121·8	9	8·40	213·5	4	8·0	114·1	12	6·99	177·1	18	6·42	92·0	13	6·55	166·7	11
9·40	131·6	3	9·50	234·0	1	8·50	120·5	30	7·25	182·7	7	7·00	99·9	34	7·02	179·4	32
10·03	138·6	3	15·40	372·0	1	9·06	126·8	5	7·96	200·6	5	7·30	104·2	27	7·36	183·9	8
11·75	161·5	2	16·95	405·5	2	9·72	134·8	5	8·51	212·9	10	7·99	112·6	15	8·12	205·6	14
15·40	209·0	1	17·70	427·8	5	10·27	140·2	4	9·55	237·0	2	8·38	118·4	48	8·47	212·2	15
16·80	228·0	5	18·35	436·5	4	11·13	152·0	3	10·13	248·0	3	8·88	123·8	31	9·14	229·0	5
17·70	237·1	5	19·0	458·0	1	11·84	163·2	5	11·2	270·0	1	9·33	130·7	8	9·70	240·9	9
18·30	243·0	5	19·6	461·0	1	13·7	189·0	1	15·46	372·2	5	9·99	138·9	16	10·24	252·4	5
19·20	253·2	6	20·36	478·0	3	15·47	208·0	6	16·77	404·0	4	11·51	158·4	7	11·33	275·6	3
19·80	260·3	3	20·80	495·0	1	16·8	224·7	7	17·63	426·3	3	12·02	163·5	4	12·05	290·5	2
20·30	265·5	4				17·77	236·8	10	18·07	432·9	9	15·41	206·9	13	15·4	368·6	5
20·9	271·9	4				18·16	242·0	6	18·65	443·0	2	16·8	224·8	9	16·8	404·1	8
						19·15	252·3	7	19·5	463·0	1	17·5	232·1	16	17·47	420·0	8
						19·6	256·0	7	20·13	475·0	3	17·96	236·2	19	17·91	427·1	8
						20·83	269·0	12	20·86	490·4	5	18·50	241·0	6	18·33	433·2	11
												19·11	250·0	12	18·98	451·2	5
												19·5	252·3	7	19·4	456·6	3
												20·02	257·7	9	20·2	470·0	11
												20·6	263·6	25	20·73	481·1	14

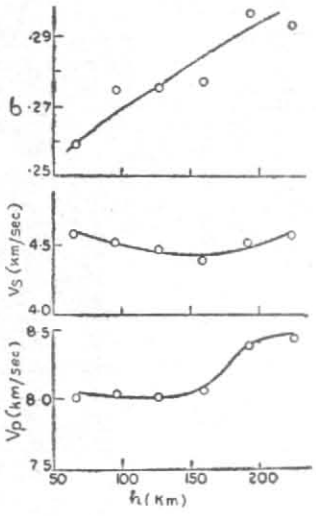

Fig. 2

of incidence arrive on the other two branches which lie overlapping the first branch. They showed that the properties of the low velocity layer could be inferred from the point of termination of the first curve and the offset time between the two curves. An overlapping of the two curves indicated a rapid increase in velocity below the channel and a separation between the curves a gentle velocity gradient.

The present study deals with the part of the ray beyond the point of deepest penetration, and the results also indicate an offset in the reduced travel-time curves both for P and S waves at a value of $\triangle$ between 12° to 15°. This together with the rapid increase in the velocity of P waves at a depth of 150 km would preclude the existence of a shadow zone. In the case of S waves, however, the velocity increases at least upto 225 km is not large and the velocity decrease below the Mohorovicic discontinuity exceeds in some portion of the channel the critical value given by Eq. 4. The existence of a shadow zone for S between $\triangle = 10°$ to $\triangle = 16°$ cannot be ruled out. Observations of the channel wave for S (Caloi-wave) in many parts of the world also confirm this view. The corresponding wave for P is not so clearly observed.

TABLE 3

h/R	Apparent velocity (km/sec)		True velocity (km/sec)		Poisson's ratio
	P	S	P	S	
·005	8·05	4·59	8·01	4·57	·259
·01	8·11	4·56	8·03	4·52	·274
·015	8·14	4·55	8·02	4·47	·275
·02	8·23	4·53	8·07	4·44	·276
·025	8·61	4·63	8·40	4·52	·296
·030	8·71	4·71	8·45	4·57	·293

REFERENCES

Dowling, J. and Nuttli, O. 1964 *Bull. seismol. Soc. Amer.*, **54**, 1981-1996.

Guntenberg, B. 1953 *Ibid.*, **43**, pp. 223-232.

Reznichenco, Y. V. and Kosminskaya, I. P. 1964 *Research in Geophysics*, **2**, Solid Earth and Interface Phenomenon, The MIT Press, Cambridge, Mass., pp. 81-122.